FERMILAB-PUB-08-697-AD

A model of rf breakdown arcs

Z. Insepov, J. Norem*
Argonne National Laboratory, Argonne, IL 60439 USA

A. Bross, A. Moretti, Z. Qian
Fermilab, Batavia, IL 60510 USA

Y. Torun, D. Huang
Illinois Institute of Technology, Chicago, IL, 60616 USA

R. A. Rimmer
Jefferson Laboratory, Newport News Virginia, 23606, USA

S. Mahalingam, S. Veitzer
Tech-X Corp., Boulder, CO, 80303 USA
(Dated: September 5, 2008)

This paper presents a first iteration of a model that attempts to describe all aspects of breakdown in rf cavities and provides some estimates of the parameters and parameter ranges involved, as an aid to producing more precise models and more useful experiments. The model describes how breakdown events can be triggered, how they grow, it identifies the power source for their rapid growth, mechanisms that limit their growth, how they are extinguished and how they can be mitigated. We also discuss applications to superconducting rf and high pressure gas structures. The model relies heavily on previous experiments with 805 and 201 MHz warm copper cavities, and preliminary plasma modeling using the code OOPIC Pro. We compare estimates from the model with experimental data where this is possible. Because of the geometrical dependence of all parameters, the wide range of experiments being performed, the wide range of experimental parameters in a given breakdown event and the lack of extensive systematic parameter searches at this stage in our studies, it is difficult to present precise results. We are constrained to showing what mechanisms are involved, the strength of these mechanisms and how they interact to produce the experimental data. We are primarily interested in the development and dynamics of the arc, magnetic and gas effects and insights on how to avoid arcing in all environments.

PACS numbers: 29.17.+w, 52.80.Vp

I. INTRODUCTION

Vacuum breakdown seems to be the primary limitation in the design and construction of high energy accelerators operating with warm (copper) accelerating structures such as muon colliders, neutrino factories, or the CLIC linear collider design [1–4]. The mechanisms that cause breakdown are also relevant to the environment that exists in superconducting rf systems such as the International Linear Collider design [5]. The physics and the mechanisms that cause this phenomenon are, however, comparatively unexplored.

Vacuum breakdown has a long history. Starting with experiments done over 100 years ago by Earhart, Hobbs, Michelson and Millikan that first defined the process, and initial modeling by Lord Kelvin, to the present day, an enormous number of papers have been published, exploring all the experimentally accessible variables [6–10]. Nevertheless, there still seems to be some uncertainty about both the overall process and many of the experimental details [11–17]. To a large extent, this is due to the fact that events occur very rapidly, during which experimental parameters vary over many orders of magnitude and a large variety of mechanisms seem to be involved. Among the behaviors that need an explanation is how these structures can operate for very long periods *without* breaking down.

This paper describes a model where breakdown is triggered by mechanical failure of a surface asperity, causing a charged plasma arc to form that can further heat the surface causing more metal and ionizing currents in an avalanche mechanism. This plasma can then produce sufficient electron currents to short the cavity, discharging the cavity energy into the wall. The electron beams, along with the arc, whose dimensions are estimated at tens of μm, can both damage the wall. The discharge is usually terminated when the drive power is removed from the cavity.

As a first iteration of a complete model we want to be able to: 1) provide explanations for all phenomena that are seen in breakdown events, 2) provide alternatives and some justification for the selection for one mechanism over another and, 3) give numerical examples and

*Electronic address: norem@anl.gov

quantitative estimates wherever possible. We hope this model would inspire more detailed modeling and iteratively guide an experimental program which could converge on more detailed aspects of the problem such as the variety of surface damage seen, transmitted and reflected power histories, frequency dependence, behavior in traveling and standing wave cavities, and the dependence of breakdown parameters on a large variety of input parameters. We do not regard this model as an end point for our own work.

In section II, we discuss some of the relevant mechanisms that operate in a high gradient environment. In Section III we describe the trigger mechanism that seems to explain how breakdown events are initiated. We believe that the "missing link" in breakdown models has been an explanation of how an event moves from a trigger mechanism, which may involve the motion of a few atoms on the nanoscale, to a multi-megawatt event a few ns later. We argue in Section IV that a positively charged plasma close to an asperity can produce enormous local electric fields capable of driving very fast growth of the arc. Section V describes some mechanisms which can control and limit the arc parameters. In the remaining half of the paper we explain how this model relates to the variety of experimental data. Experimental measurements which support this model of arc growth are are discussed in Section VI. Section VII describes the effects of an external magnetic field on the development of the arc. In section VIII we describe how this model explains the behavior of structures filled with high pressure gas such as air or SF_6. Section IX describes mechanisms that terminate the arc. Section X describes how pulsed heating in copper structures can cause breakdown events even though these mechanisms occur far from the regions of high electric fields. The relation between the normal conducting systems and superconducting rf is described in Section XI, and Section XII describes how this model would guide an experimental program to eliminate breakdown. Section XIII considers some similarities between rf breakdown and breakdown in DC arcs. An earlier paper considered how surface damage and the stored energy in the rf structure determine much of the behavior of the system [18].

We primarily present experimental data from our own experimental program, and the literature, to compare with this model where possible . The primary rf structure used in our experiments has been an 805 MHz pillbox structure, which has a stored energy of about 1 J, operating in the MuCool Test Area at Fermilab. Many of the mechanisms described here may, however, depend to some degree on cavity geometry and size, so the model may require some extension for different geometries [18]. Modeling has been done with OOPIC Pro [19] and VORPAL [20, 21]. Because of the extreme geometrical dependence of all the parameters, the wide range of experiments being performed, the wide range of experimental parameters in a given breakdown event and the lack of extensive systematic parameter searches at this stage in our studies, it is difficult to present precise results. We are constrained to showing what mechanisms are involved, the strength of these mechanisms and how they interact and some preliminary results. We feel that a coherent picture of how these mechanisms interact serves a useful purpose and justifies this paper.

FIG. 1: The three stages in breakdown: fracture, ionization, and arc development.

II. PARAMETERS AND MECHANISMS

The environment of a breakdown site is extreme in a number of parameters. Measurements show that the local electric fields are in the range of 7 - 10 GV/m, leading to field emission [22, 23] current densities in the range of $10^{10} - 10^{12}$ A/m^2 and tensile stresses exerted by the electric fields are in the range 200 - 400 MPa, comparable to surface tension forces in liquid metals, described below. These stresses are produced at a frequency of $2f_{rf}$, since the stress is proportional to E^2. In this environment it is not unexpected that materials can occasionally fail.

The properties of the breakdown arc are determined by a number of mechanisms, many of these have discontinuities around 10 GV/m. The arc itself seems to consist of a metal plasma which, at least initially, derives most of its energy from field emitted electrons from asperities on the wall. At these field levels, tensile stress is comparable to tensile strength and metallic clusters are known to be unstable to Coulomb explosions [24, 25], field emission densities are comparable to space charge limits and highly dependent on surface properties such as crystal orientation. Field ion evaporation of metal atoms can occur, and local power levels are high enough to melt or vaporize metals. The properties of these metals, such as tensile strength and resistivity, will change also with temperature. While field emission is, theoretically, a simple relation between local field and induced current, this relation is complicated by both the properties of the material, the surface, the history of the emitter and details of the emitter geometry through material failure, fatigue or space charge limits on currents and other variables.

In the simplest models, tensile stresses driven by electric fields can cause failure when these stresses exceed the tensile strength of the material. Cyclic fatigue aggravates this failure. Nevertheless, because the small size of the asperities involved, they may be relatively defect free and thus have a tensile strength much larger than the macroscopic value usually measured and tabulated, as is seen in Atom Probe Tomography samples [18].

A. Field Emission and Space Charge

Field emission has been extensively studied both as a diagnostic tool to measure the local electric field and as a stressing mechanism. Any small radius asperity can, in principle, produce field emission electrons that would be accelerated by the existing cavity fields. With a knowledge or estimate of the effective local work function, ϕ, it is possible to make an estimate of the local electric field on the surface of asperities. This has been extensively documented in other papers [26, 27].

Although field emission depends on the work function, this dependence is not simple, since ϕ can depend strongly on submonolayer surface coatings (contamination) and even crystal orientation on the nanoscale. Barbour et. al. [28] have measured the dependence on both of these parameters with detailed photographs of the surface through field emission currents that clearly show how some faces of a generally hemispherical emitter are strongly emitting while other surfaces, a few atoms away, are not visibly emitting. These difficulties are generally not considered to be significant modifications of the models, but they can have a substantial effect on the field emission current.

Under some circumstances, the power produced in field emitted beams can be limited by the space charge limit. This limit arises because dense electron beams can contain sufficient charge to affect the electric fields that accelerate these beams. The effects of the space charge limit on field emitting surfaces have also been documented by Barbour et. al. [28], who used tungsten needles in a spherical chamber and measured this limit as

$$j_{[A/m^2]} = 5 \times 10^{10} (E_{[V/m]}/10^9)^{3/2},$$

for surfaces with a variety of work functions, controlled by submonolayer additions of different materials. Barbour et. al. imply that all field emitters would see the space charge limit below 5 GV/m. This is inconsistent with many measurements on rf cavities which show emitters operating at almost twice that field [26].

Although the space charge limit has been important in the design of vacuum tubes with a variety of geometries., it has usually been calculated for geometries (planar, cylindrical and spherical) where the problem is essentially one dimensional, in that the electric fields produced by the beam charge directly add or subtract from the electric field driving the current. The geometry of the field emitters we are concerned with in this paper, however, are small hemispherical surfaces emitting currents into a rectangular environment, where, once away from the emitter, the electric fields produced by the beam can extend perpendicular to the accelerating fields, reducing the beam density and the space charge effects. Thus the common values of the space charge limit do not apply and the limit must be determined by numerical modeling

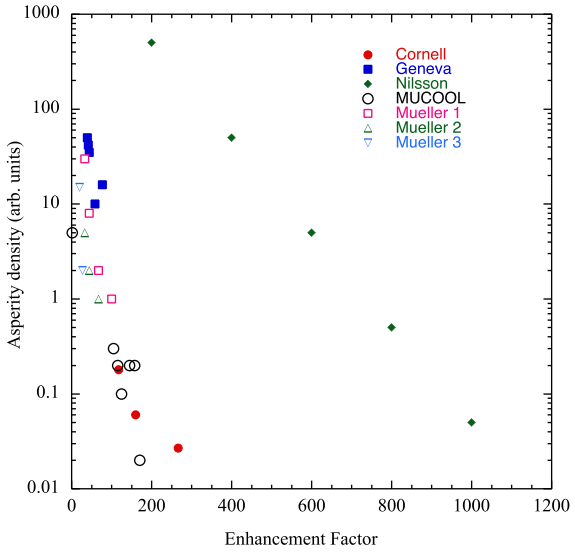

FIG. 2: The spectrum of enhancements in various "clean" and "damaged" surfaces. This data is presented in the style of Nilsson [30] and includes data from References [30–33, 35].

B. The Surface

We are not concerned in this paper with the exact geometry of emitters. We do however want to understand the nature of field enhancements and the spectrum of field enhancements present in operating cavities.

A simple explanation for the local enhancements of the electric field has been given by Feynman, as part of an explanation for gas breakdown that is completely relevant to this problem [29]. We assume that the $1/r$ dependence is the result of a statistical fluctuation producing a small equivalent three dimensional radius r at grain boundaries, defects, or sources of contamination.

There is considerable experimental data on the distribution of the surface asperities that cause field emission obtained both from working rf systems and from extensive measurements with field emission microscopes. Many examples of this are included in the literature, see Fig 2 [30–32, 35]. By studying the number density of visible emitters while altering the electric field, one can deduce the emitter density as a function of electric field. Although the different types of data are not normalized to each other, they all seem roughly consistent with a parameterization of the form $f(\beta) = exp(-D\beta)$, where β is the enhancement factor, defined in terms of the local field at the asperity divided by the average surface field, $\beta = E_{local}/E_{av.}$, and D is a numerical constant [30–33]. The data obtained by Nilsson was the result of a technique designed to produce a distribution of high enhancement factors [30]

III. BREAKDOWN TRIGGERS

In this paper, we assume that neutral material can be injected into the region above a field emitter to trigger the breakdown event. In order to explore the nature of the trigger process, we consider two options for the neutral injection mechanism, fracture and melting, although other mechanisms exist. The strongest argument for fracture seems to be that breakdown thresholds appear to be statistically driven, generally exhibiting fatigue behavior, while Ohmic heating is highly dependent on the geometry of the asperity and is a more complex process. Needles and shallow cones can have the same surface field, but ohmic heating and thermal conductivity can vary widely from example to example. We know that cavities seem to operate with about 7 GV/m local fields, which would not be predicted by Ohmic heating, unless all asperities had identical geometries [26]. The Ohmic model was completely described 55 years ago, in papers by Dyke et. al. [34].

A. Fracture

The primary problem is to identify the mechanism that can inject neutral or ionized material into the region above the field emitter, where it can be ionized. The high local fields implied by field emission spectra ($E \sim 10$ GV/m) also imply tensile stresses, $T = \epsilon_0 E^2/2$, in the range of 400 MPa, which would be an element in any trigger mechanism, and perhaps the simplest of all mechanisms to describe. A model of a breakdown trigger based on tensile stress has been previously documented in the literature [18, 26]. The basic mechanism is related to both Coulomb explosions of materials and fatigue failure under tensile stress [25]. In previous papers we have suggested the tensile stress caused by electric fields as the primary cause of the mechanical failure of the surface.

It is well known that when metallic clusters and molecules are highly charged, electrostatic forces can cause them to break apart. These Coulomb explosions can also occur when the electrostatic properties of molecules or clusters have been altered, perhaps by laser ionization, so that the electrostatic repulsion is greater than the binding forces and this repulsion can cause them to burst apart, producing charged and very energetic ions, fragments, x-rays and high energy (keV) electrons [24, 25]. This process occurs at surface electric fields of around 10 GV/m, the local surface field where we expect that tensile stresses are comparable to the tensile strength of cavity materials. While the phenomena of charged clusters breaking up due to laser ionization and metal surfaces fragmenting due to applied electric fields are different, the surface environments seem identical. For structures with radii from 10 nm to 100 nm, the electron excess or deficiency required to do this is on the order of 0.001 to 0.01 charges per atom. The mechanism of Coulomb explosions can occur in at least two contexts: 1) the initial fracture of the surface itself, and, 2) the breakup of fragments produced by fracture of surfaces in the presence of electron currents, which seems to be exactly the same phenomenon.

Fatigue seems to be involved in the failure mechanism since asperities can operate for a long time with stable operation before failing. The relationship between failure rate and electric field is proportional to a high power of the electric field, which seems to follow the laws of fatigue failure. The Wöhler curve describes how the applied stress on a component affects the lifetime of that component [36]. Thus we expect that the electric field, and the stress it causes, is related to the breakdown rate.

While fatigue failure may explain the breakdown rate as a function of field, fatigue is primarily defined for macroscopic obects. The phenomenon of creep, where defects move in materials which are subject to cyclic loads, can be used explain how the cyclic stress affects materials and causes fatigue-like effects on nanoscale objects. Tensile stress driven fracture at these fields is modeled by Z. Insepov using a molecular dynamics program, showing how the electric field draws atoms carrying excess induced charges out of the material, see Fig. 3 [37, 38]. Creep, which draws lattice defects towards areas of higher stress creates some cumulative damage in the material by creating points where the material can yield.

While it is difficult to analytically estimate the minimum size of a fragment or cluster that could trigger a macroscopic breakdown even, OOPIC Pro simulations have shown there is a critical mass density (35 Torr) for the copper gas above an asperity, below which the rate of ion production via impact ionization is insufficient to produce a sustainable plasma, in which case there is no breakdown event. This effect seems to define a threshold for the minimum perturbation which can trigger a breakdown event. We expect this threshold may be material, geometry and field dependent. The dependence of this process on electric field is ultimately determined by the creep mechanism, where defects move in asperities as a function of stress, as shown in Fig. 4.

B. Melting

The Fowler-Nordheim model seems to allow almost arbitrarily large current densities at asperities, and it seems straightforward that at some density the ohmic heating would cause melting. In addition, Dyke, Trolan et. al. argued that for tungsten needles that see pulsed field emission current, melting does in fact take place [34]. Nevertheless, the ratio of Ohmic heating to thermal conduction of this heat away from the hot spot is highly geometry dependent. Needles, like those used by Dyke and Trolan et. al., produce the most Ohmic heating while conducting away the least. Sharp, low angle cones, which we think are more characteristic of breakdown sites, would produce much less heating and conduct it away much better.

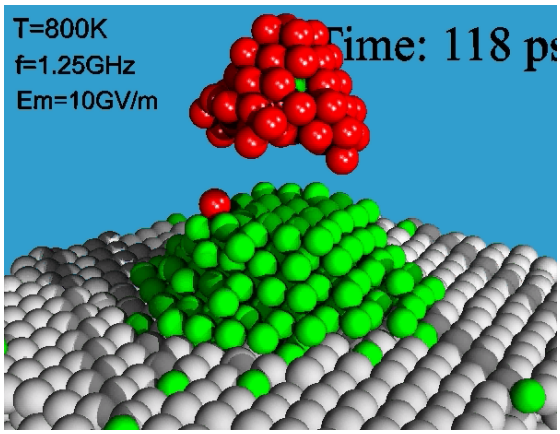

FIG. 3: Surface fracture at high electric fields, as modeled by Molecular Dynamics. The figure shows a cluster of charged atoms being pulled off the top of an asperity by a 10 GV/m electric field. This mechanism is described in more detail in an earlier paper [37]. This process seems to be similar to Coulomb explosions of clusters, and the fragments produced may themselves be broken up by Coulomb explosions.

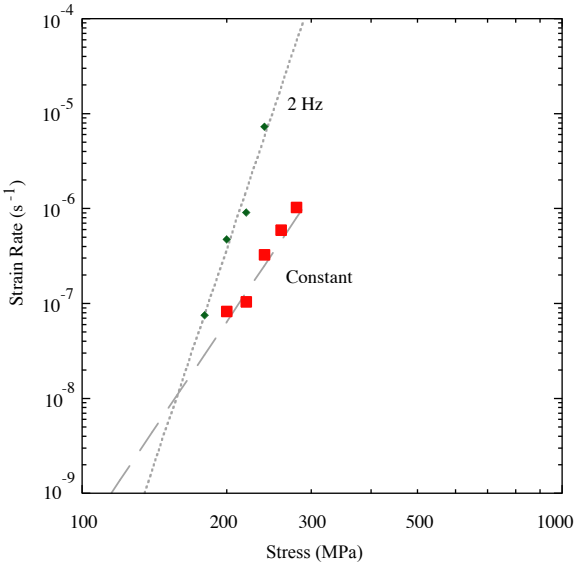

FIG. 4: Plot of strain rate vs. stress for a model of defect motion due to creep. We assume that fatigue failure in asperities is due to motion of these defects and would be governed by this stress/strain relation [36, 38].

In the absence of a strong electric tensile stress, most phenomena active in high power environments, such as field evaporation and surface tension, would tend to make surfaces smoother. As materials are heated to melting, surface tension on small perturbations can become a very strong force. Field ion evaporation will also tend to increase the radii of surfaces under high fields along with the cluster or ion impacts from gas molecules.

While melting is not required in the initial breakdown trigger, we expect meltng in the subsequent development of the arc. There is ample evidence for melting during the high power phase of the breakdown process. Tensile stresses, combined with ohmic heating and intense surface bombardment from electrons and ions will tend to pull the metal surface to form sharp cones, where intense ohmic heating due to field emitted currents can further increase the temperature of the metal.

C. Other mechanisms

There are a large number of other mechanisms that could trigger release of metal from the surface. We expect metals to have surface oxides and these oxides complicate any surface process in a number of ways. They would be more resistive, thus producing more ohmic heating, and they are generally harder, thus there would be cyclic stresses from differential expansion due to tensile stresses. The properties of metals, such as resistivity and tensile strength, will change with temperature. Defects will migrate inside an asperity and surface ion migration could occur which changes the morphology of the surface material. Outgassing could be driven by tensile stresses or surface strain. Sequential plastic deformation could occur due to cyclic heating and tensile stresses. Solute segregation could change the nature of grain boundaries. Unfortunately, experimental data is very limited and it is difficult to study all the combinations of processes that could contribute, so we argue that tensile stresses alone provide a useful trigger mechanism.

Cause and effect are also difficult to separate. Microphotographs of cavity structures at CERN show highly deformed material, with many cones, cracks and a variety of other microstructures on the surface that seem to be a result of the high gradient environment [39]. While these could of course be potential breakdown sites, they could also be comparatively benign damage caused by heating from many previous breakdown events. We believe that breakdown events are accompanied by very high levels of UV and x-radiation which come from the high density copper plasmas described below. A recent paper has discussed the equilibrium that exists between surface damage and high gradient operation of structures [18].

We assume that the precise nature of the trigger is, to some extent, unknown. Fracture followed by ionization is a simple process that is easy to quantify and seems to explain all the experimental data, thus we are not concerned in this paper with alternative mechanisms. Atom Probe Tomography, (APT), which studies materials at very high positive surface potentials, sees materials fracture, but does not see significant motion of surface atoms or gas production in 1 - 50 M pulses at $\sim$ 10 GV/m field levels [18, 40]. Ultimately, however, all alternative mechanisms outlined above are caused by the same local surface fields and are indistinguishable after the arc begins.

D. Ionizing the atomic cloud

We assume that the trigger for breakdown events is the injection of high density material above a field emitter, where the intense, energetic currents would break up and ionize the material to produce a plasma. A number of mechanisms could be involved. Coulomb explosions could result from either ionization or electron absorption of field emitted electrons by clusters. Lord Rayleigh showed that when the electrostatic energy becomes comparable with the binding energy of the cluster, it can become unstable [41]. The number of charges involved in charging up small (10 - 100 nm) clusters is not large, perhaps 1000 electrons, a small fraction of the $\sim$ 6 M electrons/ns field emitted in a 1 mA current. We expect that the Coulomb explosion process would be sequential, until the solid material is reduced to atoms.

The dimensions of asperities have not been directly measured but seem to be approximately 50 nm radius [26]. Thus we would expect that the electron energy for the field emitted beams would be in the range $eV = e(E = 10 \text{ GV/m})(dr = 50 \text{ nm}) = 100 - 1000$ eV. Electrons of this energy have a range on the order of a few nm in Cu. Thus all the energy would be deposited in small clusters.

Ionization of neutral metallic gas has been modeled by OOPIC Pro assuming field emitted electrons are produced below an inirtially confined atomic gas [20]. Initial results show that the ionized electrons, as well as the majority of the field emitted electrons, are accelerated through the plasma producing a net positively charged plasma which is slowly accelerated towards the surface.

E. Modeling with OOPIC Pro

OOOIC Pro is a particle-in-cell physics simulation for 2D (x, y) and (r, z) geometries with 3D electrostatic and electromagnetic field solvers and Monte Carlo collision and ionization models. The code operates on many platforms and has a useful user interface [20].

In order to study the breakdown process in a simple way we have modeled a geometry where a cylindrical cloud of neutral copper gas 2 μm thick is suspended inertially 1 μm over a field emitting asperity as shown in Fig 5a. The copper gas models a copper fragment broken off the tip of an asperity. The dimensions of the conical asperity are 2 μm in height and 4 μm in diameter at the base in order to localize the plasma. Such conical asperities, while not unphysical, are not a necessary component of the model, but useful for computational purposes. We assume that a field emitter is located on the surface of this asperity such that the enhancement factor of the combined system is 184 [26]. OOPIC Pro models field emission at high current densities in a self consistent way by calculating space charge fields from the emitted electrons in the presence of whatever plasma ions and electrons are in the immediate area. The ionization of copper and various secondary emission coefficients are contained in the code [19]. The grid size for these initial runs is set at 200 nm, and the time step is set at 10^{-14} sec which seems adequate for plasmas whose dimensions are $\sim$ 10 μm.

Since the OOPIC Pro code has been used in a number of different applications and has been benchmarked against other codes, the initial aim of this preliminary effort was to calculate radiative losses due to line and continuum radiation, to understand the complete spectrum of heat flux on the wall.

Although the code cannot yet follow the many orders of magnitude changes in density and current, it seems to be fully functional in its ability to provide a description of the first 5 ns of a discharge, giving the plasma dimensions, densities, electron and ion temperatures, power fluxes to the wall due to ions and photons. We are developing a more integrated way of providing a complete description of the initial stages of the plasma (time constants for density growth, etc.) during the critical, first few rf periods, as well as modeling magnetic fields with different strengths and intensities. The

The plasma we describe has some similarities with unipolar arcs, a fairly common phenomenon seen in tokamaks [42]. The difference between the rf and tokamak environment, however, is the high gradient electric field that sweeps away many of the plasma electrons and produces the potential between the plasma and the wall, so that the tensile stresses, field emitted currents, ion motion and power levels are no longer quasi stable, but rapidly increasing. Electron return currents are not a significant component of the rf arc and the plasma is strongly bipolar and asymmetric.

IV. ARC DEVELOPMENT

Modeling with OOPIC Pro shows the basic mechanisms that operate in a metallic plasma in a high gradient environment driven by field emission from a nearby source. Electrons are swept away from the ions by the background E field, leaving a positively charged cloud of relatively slow moving ions, see Fig 5b. The net effect is to increase the surface gradient seen at the asperity, increasing the field emission current and tensile stresses by large factors. Since this gradient increase occurs in the presence of significant UV and ion surface heating we assume that the surface would melt. Power levels and other parameters are discussed below. We would expect significant fluxes of sputtered ions and secondary emitted electrons.

There are a number of mechanisms that are involved in the development of breakdown events in an rf cavity. These are shown in Figure 6. We assume the arc development will proceed in the following stages: 1) the arc is initiated by a fragment or cluster broken off of a field emitter, as described in section III, 2) the fragment is then ionized by field emitted beams to form a plasma,

3) the electric field around the arc will pull and accelerate electrons out of the plasma, charging it up, and producing bremsstrahlung x-rays when the electrons hit the far wall, 4) the positively charged plasma above the asperity will increase the electric potential on the asperity causing increased field emission and ohmic heating which should melt the asperity so that the much larger tensile stresses should further increase the flux of metallic atoms and ions into the plasma, along with secondary electrons. This will cause: increased surface heating in the form of 5) ion bombardment and 6) line radiation (x-rays) from the plasma which will further heat the surface. The plasma will also see contributions from 7) secondary electrons. As the plasma develops and the rf electric field changes sign, the surface will also see a bombardment of 8) plasma electrons. The whole cavity will be subjected to a flux of 9) intense line radiation and 10) atoms and ions from the plasma which will cause damage, likely to initiate the next breakdown event. In this paper we assume that the high power levels of relativistic electrons hitting the far wall are diffused over a fairly large area and does not significantly contribute to the development of the arc. The primary mechanism for the breakdown process to absorb the cavity energy is the acceleration of plasma electrons to the opposite wall of the cavity.

As an example of the time development of the plasma we show, in Fig. 7, an OOPIC simulation of the flux of line radiation on the asperity in the early stages of a discharge. The ionization state would be determined from coronal equilibrium, for a given electron energy and atomic species [43]. As the plasma develops with time, the densities of both the electrons and ions increase, and the line radiation, which is proportional to the product of the two densities, also increases. The generation of a dense plasma would require a significant time before measurable currents could be generated and the breakdown event could be externally detected from the loss of cavity energy. Figure 7 shows a roughly exponential growth of the plasma density (the square root of the radiation level) with a time constant on the order of one ns. Fig. 7 also shows the dependence of the discharge on magnetic fields, which we will describe in more detail below.

The "impurity radiation" shown in Fig. 7 comes from two sources: line radiation, proportional to $n_i n_e T_e^{-1/2}$, and continuum radiation, proportional to $n_i n_e T_e^{1/2}$, where n_i, n_e and T_e are the ion, electron densities and electron temperature. At the low temperatures predicted by the model, line radiation dominates. This data is preliminary and does not include reabsorption, screening and plasma cutoff effects, which will be added.

While the mechanism we describe is somewhat similar to Explosive Electron Emission (EEE) [14], the rf environment, with essentially pulsed fields, is somewhat different from a DC or single pulse case where the driving field is always present in the initial stages of the discharge. We argue that the growth of the plasma in the rf environment is essentially exponential at all times, although the growth time should depend on the immediate environment of the asperity.

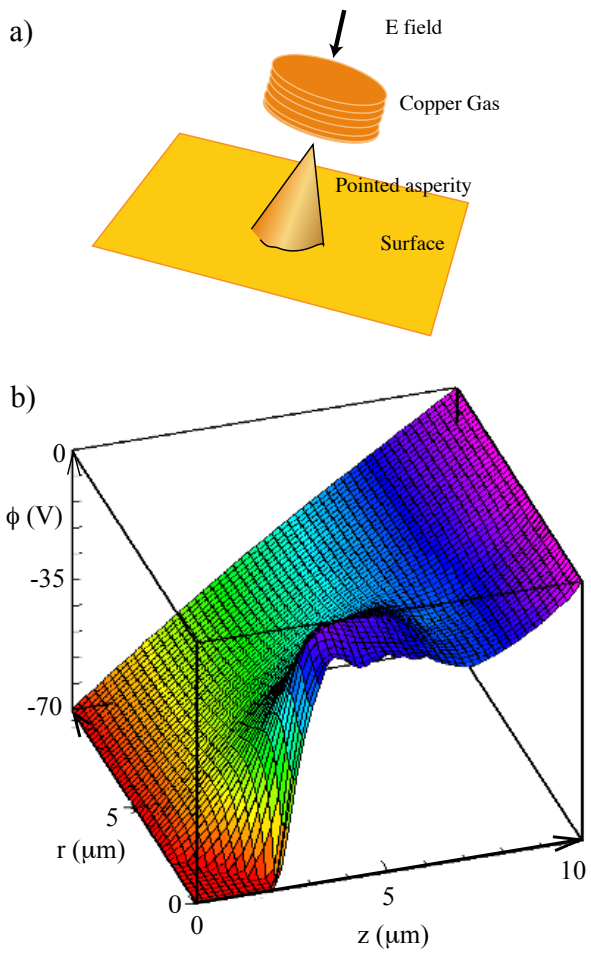

FIG. 5: a) The basic geometry used in these calculations: an asperity field emits electrons into a copper gas. b) OOPIC Pro results showing the scaler potential ϕ as a function of r and z, in the region of an asperity located at $r = 0$ and $z = 0$ on the $z = 0$ surface. The plot shows how the surface electric field, the slope of the potential, $E_z = d\phi/dz$ is amplified by the positively charged plasma that forms over the asperity. The effect of the plasma formation is to almost immediately increase the local electric field at the breakdown site by a large factor over the field, $E_{local} = \beta E_{surf}$ ~7 GV/m, with $\beta = 180$, that caused the initial breakdown trigger.

V. LIMITING MECHANISMS

There are many uncertainties in the development of a breakdown event but the process can be controlled by a relatively small number of mechanisms that can be isolated and studied separately. Among the factors which seem to be critical to the development and overall parameters of the plasma, are: 1) the maximum allowable field emission current, which seems to determine the power

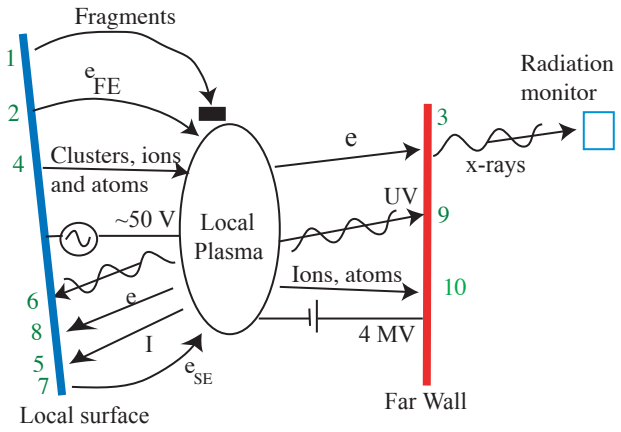

FIG. 6: Energy and particle flows during breakdown. We assume that the process is initiated by the production of fragments that are heated and ionized by field emitted electrons, producing a plasma whose electrons can be accelerated to the far wall to short the cavity fields. The dimensions of the plasma are on the order of 10s of μm, with an electron tail extending to the far wall.

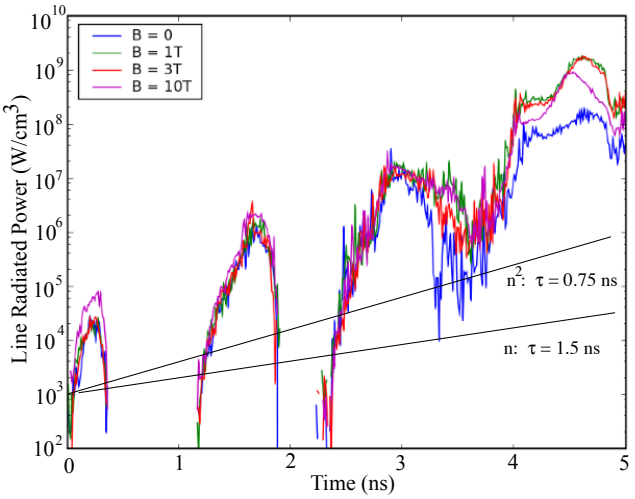

FIG. 7: OOPIC pro modeling of impurity radiation in the initial few rf cycles at 805 MHz. The radiation is produced by a relatively low temperature Cu plasma, and the intensity is proportional to the product of the election and ion densities, $n_e n_I$. The radiation grows with a time constant of $\tau \sim 0.75$ ns, and the density grows with a time constant of ~ 1.5 ns

going into the plasma, and thus most of the parameters of the arc, 2) the relativistic electron optics and electron shower dynamics which determine how most of the electromagnetic energy of the cavity is converted to heat, and, 3) the dynamics of the metallic injection process by which metal is fed into the plasma which determines how an arc can be maintained in equilibrium with the electromagnetic field.

A. Field Emission Limits

This model of the breakdown arc assumes that the arc plasma which develops over the original asperity derives the majority of its power from field emission electrons which interact with the metallic plasma. This plasma then produces fluxes of UV radiation, ions and hot atoms which further heat (melt) the wall, which causes liquid metal to be injected into the plasma. The plasma parameters are probably determined by the balance of electrons (heating) and metal (cooling) entering the plasma. We would expect this balance to produce a relatively cool plasma. The flux of field emission electrons is limited by the space charge limit for the appropriate geometry. The power radiated as impurity radiation from the plasma would be limited by the overall energy balance of the plasma, thus also by field emission of electrons and space charge.

Field emission from hot materials has been described analytically by Jensen [44], however the primary limitation on the current seems to be due to space charge from a number of plasma species in motion in the immediate region above the field emitting surface, and this space charge limit is most easily evaluated numerically. The complex interactions of the plasma and the wall also seem to require modeling to understand the details of the process. More detailed calculations are underway using OOPIC Pro and VORPAL [19–21].

B. Relativistic electron dynamics

The major energy loss mechanism for the cavity would be expected to be the flux of plasma (field emitted, ionization and secondary emission) electrons which are accelerated to relativistic energies into the opposite wall by the cavity fields. We expect electron currents could exceed a few amps, limited by space charge, and be accelerated to energies of a few MeV, depending on the geometry of the cavity, thus amounting to power levels of a few MW.

Accelerator cavities operate at average gradients up to $\sim$ 100 MeV/m. The cavity resonance then produces B fields on the order of $B = E/c \sim 0.3$ T, where c is the speed of light. Since the relativistic electrons are produced around E_{max}, the field is changing at a rate of $dB/dt = B\omega$, and the plasma may produce electrons for approximately 1/4 of an rf cycle, roughly $\delta t = 1/\omega$. As a numerical example, 4 MeV electrons have a rigidity of about 0.2 Tm, and might be spread over a length, giving $dr \sim 1$ cm.

We will show below that breakdown events in our pillbox cavity produce fluxes of about 4 MW of relativistic electrons to the opposite wall of the cavity. Modeling shows that these electrons are emitted from the plasma very close to the surface. Since the potential difference between the walls of the cavity E_{max} is about 4 MV, we would expect these relativistic electrons to represent

currents on the order of a few Amps.

The distribution of the power once the electron beam enters the metal is governed by well understood models of low energy showers which depend on the energy of the electrons and the material [45]. The deposited energy per unit volume is low at the surface and increases with depth as the electron gives energy to secondary particles.

During the arc, electrons accelerated to the far wall can efficiently remove power from the cavity if the transit time of the electrons is comparable to 1/4 of the rf period. When the remaining field in the cavity is no longer able to accelerate these electrons to satisfy this condition, the cavity can no longer lose energy efficiently, and it will maintain itself at some low field level until the end of the power pulse.

The special case when there is a strong magnetic field parallel to the electric field is interesting. Under these conditions the electrons and ions are "pinned" to magnetic field lines and both field emitted electrons from normal asperities and the intense, relativistic beams from breakdown plasmas are forced to deposit all their energy in a small volume of material. The normal field emitted beams have been detected with Polaroid film and glass slides, and the much more intense beams from damage spots from breakdown events have been seen on the cavity walls and on the titanium vacuum windows, one of which burned through the metal to produce a vacuum leak. These are described in Ref [26]. Both the breakdown and field emission spots are circular. however field emission beams are better measured, since they can be predictably produced.

C. Metal Injection

There are a number of sources of heating which will raise the temperature of the asperity as the arc develops. If we assume that $\sim$ 1 A of electrons, which eventually become relativistic, leave the plasma, approximately this current of ions must also leave the plasma to be absorbed by the asperity which began the breakdown event. Modeling has shown that this flux of ions would have 30 - 60 eV of energy, representing significant power into the top few nanometers of an area of a few micrometers^2. Ohmic heating would add to the power absorbed by the asperity.

We show below that the electron energy deposited on the wall of the cavity opposite to the arc is on the order of 10 MW in our example, which with a potential difference of 4 MV, implies a current on the order of a few amps. If the plasma is to remain roughly neutral, we might expect comparable ion currents to be deposited in the arc, which with a $\sim$ 50 V potential drop would imply the $\sim$100 W of power hitting the wall at the site of the arc would heat the asperity which caused the arc. Since the thermal diffusivity of copper is equal to $D = 1.2\times10^{-4}$ m$^2/s$, this heat would diffuse $x = \sqrt{4Dt} = 1$ μm into the copper in 10 ns, very efficiently heating the asperity [46].

Injection of liquid metal, at a rate governed by the melting of an elongated tip by plasma and ohmic heating, should proceed through a mechanism similar to the electrospray of liquids by electrostatic fields. The combination of high electric fields producing tensile stresses many times the tensile strength of the material, field emission currents causing ohmic heating, and bombardment of the surface by ions and line radiation will produce a highly stressed environment on the tip of the metallic surface. We expect these would produce jets of charged clusters or liquid metal into the plasma, limited by the rate that this metal can be heated.

The surface tension of molten copper cannot be neglected. This quantity has been measured by Matsumoto et. al. to be about, $\gamma = 1200$ mN/m, slightly above the melting point [47]. The internal pressure produced by surface tension forces inside a spherical liquid with radius r is, $p = 2\gamma/r$, and this is comparable to the forces produced by 10 GV/m electric fields for radii of around 6 nm. Thus we would expect that surface tension would be important in determining both how materials melted, and also how the surface formed when liquid surfaces solidified. Setting the surface tension pressure equal to the tensile stress exerted by the electric field and solving for r, gives $r_{eq} = 4\lambda/\epsilon_0 E^2$. Liquid surfaces with larger radii would tend to be sharpened by the field and surfaces with smaller radii would tend to be dulled by surface tension.

While many parameters are comparatively hard to obtain, the total amount of metal injected into the cavity, and the energy required to melt this metal can be estimated from the size of craters seen on the irises and inside surfaces of our structures [26]. Based on the volume of metal alone, less than 0.01 J was required to remove material from the walls of a cavity which is operating at a stored energy of 2 - 4 J, which is negligible. Figures 22 and 24 in Ref [26], shows both spheres of copper on the irises of an open cell cavity, and splashes caused by balls of copper which seem to have been propelled a distance of $\sim$0.5 m to impact a thin window. The droplets are on the order of 20 μm in diameter. The splashes have the general shape of drops of solder that have fallen about 1 m to the floor. One can roughly estimate the velocity of these droplets from their even distribution across the window to be on the order of 10 m/s. Note that because the metal droplets move so slowly we expect them to be unaffected by the oscillating electric field they pass through, and so the only accelerating force they see is present at the instant they detach from the surface.

VI. CAVITY MEASUREMENTS

One of the experimental problems in studies of arcs is that most of the useful parameters vary over many orders of magnitude in a very short time. The model presented in this paper shows, however, that all the parameters of the arc are, in principle, accessible both to modeling and experimental measurement, and a detailed comparison should be very useful.

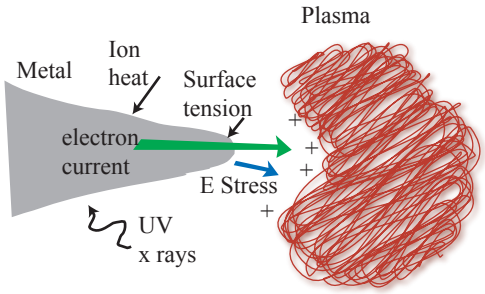

FIG. 8: Electrostatic spray of liquid materials as clusters. The electric fields and the stresses and currents it induces are many times those which originally caused fracture of an asperity. It is also likely that the dimensions are larger. Preliminary modeling has shown that the ion heating alone could produce on the order of 50 W of surface heating in an area of a few μm^2.

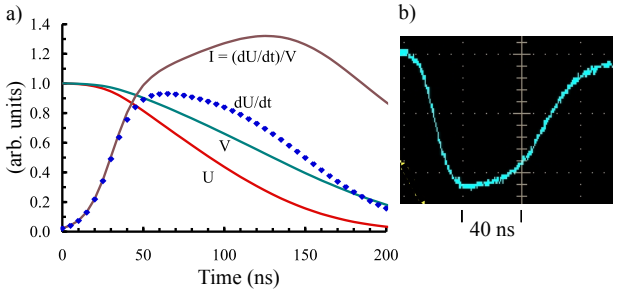

FIG. 9: a) The cavity stored energy, U, the electric field, E, the shorting current , $I = -(dU/dt)/V$ and the radiated power, $P = -dU/dt$, during a breakdown event showing $\sim$ 10 MW EM energy leaving the structure. b) The PMT trace shows the signal with 40 ns.div and 100 mV/div, using a PMT supply voltage of 900 V.

We expect that the energetics of breakdown events will depend strongly on the cavity size, frequency, stored energy, whether it is a traveling wave or standing wave and the cavity material. Unfortunately, data that could be used to compare and isolate the effects of different parameters is collected fairly nonsystematically and thus it is difficult to do parametric studies. In this paper, we primarily look at one, comparatively well studied, cavity which has been part of magnetic field studies for the muon cooling program at Fermilab [26, 27].

The power levels diverted into relativistic electrons can be measured from the x-ray radiation produced during breakdown events. Since cavities are primarily thick walled structures the energy produced will generally be the result of electron showers produced in the cavity walls, but one would expect that since the radiation length of copper is 1.43 cm, comparable to the wall thickness, a significant fraction of a shower energy would be detected by radiation monitors located around the cavity.

We have measured the energy produced during breakdown events in an 805 MHz pillbox cavity roughly 0.08 m long at about 40 MV/m gradient. At this field, the cavity contains about 1 J of electromagnetic energy. During a breakdown event, the cavity loses about half of this energy. Pits produced on the interior surface of the cavity have an average diameter of about 200 μm and depths of about 50 μm. The total energy involved in melting and removing this material from the wall, neglecting the heat lost in the wall, was about 0.02 J, a small fraction of the available energy.

We have used a scintillator photomultiplier tube assembly with the voltage turned down until breakdown signals showed some height fluctuations, insuring that the signals were not being saturated produced signals shown in Fig 9. The photomultiplier detects x-ray radiation which is presumed to be roughly proportional to the electron current accelerated across the cavity, and since this seems to be the largest source of energy loss during breakdown, we argue that this signal is proportional to the rate of energy loss of the cavity $P(t) \sim -dU/dt$. We also plot the curve that was fitted to one of these breakdown waveforms. If we integrate this signal we can produce a signal proportional to the energy in the cavity, $U(t)$, whose derivative is proportional to the electric field or energy gained by electrons crossing the cavity, $V(t) \sim \sqrt{U(t)}$. The shorting current is then $I(t) = -(dU/dt)/V(t)$. We see that this current rises exponentially in the early stages of the discharge and the time constant of this current rise should be related to the properties of the surface plasma. At least in the early stages, the plasma density is increasing with time. Note that the overall time of a 1 J breakdown event is around 200 ns, so the instantaneous power is of the order 10 MW, and assuming the electric field, E, is about 30 MV/m over a distance, d, of 0.08 m, the voltage, Ed, is on the order of 2.5 MV and the current is $I = P/V \sim 4$ A. There is some scatter in the traces of photomultiplier signals so these numbers vary by perhaps a factor of two from event to event.

We can fit the measured pulses with an expression like,

$$f(t) \sim \frac{1}{1 + exp((t - t_1)/\tau_1))} \frac{1}{1 + exp((t_2 - t)/\tau_2))},$$

where t_1 and t_2 determine the width of the pulse and τ_1 and τ_2 are the exponential rise and fall times. The exponential growth time can be determined from measurements of the leading edge of the photomultiplier pulse. We assume that the rise time can be fitted from the initial rise in the x-ray pulse. During reconditioning of the pillbox cavity, we recorded these pulse shapes and determined the time constants and the standard deviation of the distribution, these are plotted in Fig 10. The figure shows that as the gradient (stored energy) increases, the growth time becomes shorter. These measurements can be correlated with the estimates of growth times from modeling, however the plasma growth rates through the discharge are governed by different mechanisms.

It is interesting to compare the data on growth times obtained from OOPIC Pro for the first few ns of the discharge and and the photomultiplier data at the end of

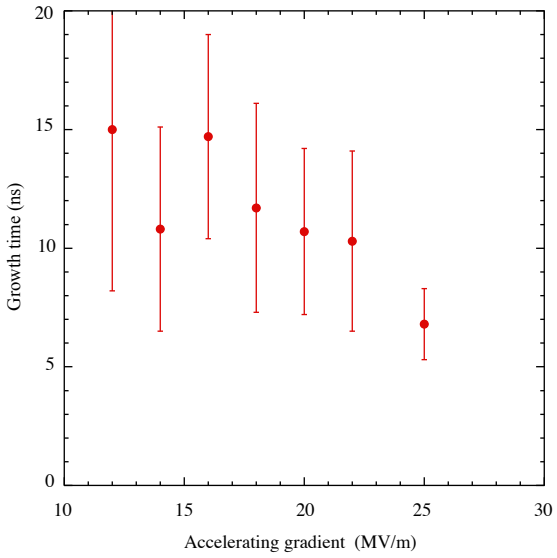

FIG. 10: This plot shows the measured growth time of the x-ray pulse as a function of the accelerating gradient. The error bars show the width (actually the standard deviation) of the distribution of rise times.

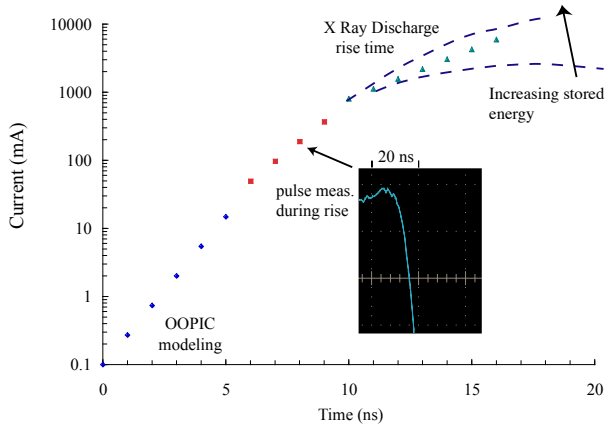

FIG. 11: This plot shows a simplified picture of the growth of the breakdown pulse. OOPIC Pro modeling (Fig 7) shows a ∼1 ns growth time in the initial plasma charge density, and measurements of the final x-ray pulse shape show a 3 - 30 ns growth time as the shorting pulse develops. On the other hand turning up the PMT gain shows growth times of ∼ 2.5 ns in the x-ray pulse before they reach full current. The vertical normalization of the OOPIC modeling is determined from measurements of electron motion, PMT data is normalized assuming a 1 J stored energy is discharged in 250 ns through a potential difference of ∼4 MV, giving A scale currents. The inset shows the ∼1.5 ns risetime seen when the PMT voltage was increased to 1200 V.

the cycle. Modeling gives an exponential growth time of about 1 ns for the initial few rf cycles. The PMT data shows that the growth times are in the range from 3 - 30 ns, with the shortest times only produced at the highest gradients. In order to extend the range of the PMT data we increased the high voltage on these tubes from 900 to 1200 V to produce more gain and look at earlier in the pulse. When this was done we obtained growth times on the order of 1.5 ns. When these data are combined on the same plot it produces the results are shown in Fig 11. We find a continuous rise in the plasma density with an initial time constant of about 1.5 ns. The growth time constant slows slightly as the discharge gets more energetic, until it finally produces the shorting electron currents that produce the x-rays, when growth times of up to 50 ns were measured..

One of the phenomena which any model of breakdown must explain is the acceleration of droplets which splash into the walls of the structure, see Fig. 22 of Ref [26]. Although these fairly large liquid drops could have some charge, they move so slowly (a few m/s) that they would not see, or be affected by, the rapidly fluctuating rf fields, and thus must obtain all their acceleration from the local plasma. In the model described here, the large tensile stress caused by the electric field between the plasma and the asperity would be responsible for the acceleration of solid or liquid masses which could fly through the plasma. Assuming a droplet of radius 50 μm, in a field of 100 - 1000 MPa tensile stress, this would produce an acceleration of 1.7×10^9 m/s^2, which could accelerate this droplet to velocities of 10 m/s, in distances of 100 - 200 nm. Particles of roughly these velocities have been seen in our structures. Although the accelerating fields are very large, the binding energy of clusters may be large enough to keep them together during the acceleration process, the energetics of this process are similar to Coulomb explosions, which require very high electric fields to break apart what are essentially surface tension forces [41].

An equilibrium seems to exist between the surface damage created in breakdown events and the maximum field that can be obtained in a given cavity. The overall influence of the surface damage left in the cavity by a breakdown event is described in Ref. [18].

A. Other Measurements

The model predicts an intense burst of UV/x-rays which would radiate from the plasma arc, as shown in Fig. 7. This radiation could produce sequential melting of the surface layers which could deform under the large tensile stresses caused by the electric fields to form a variety of surface morphologies. Many examples of curious structures have been seen at CERN in high power tests of CLIC accelerating structures. Fig. 12 shows an uncommon type of damage seen in highly stressed structures [39].

One of the clear predictions of this model is that the

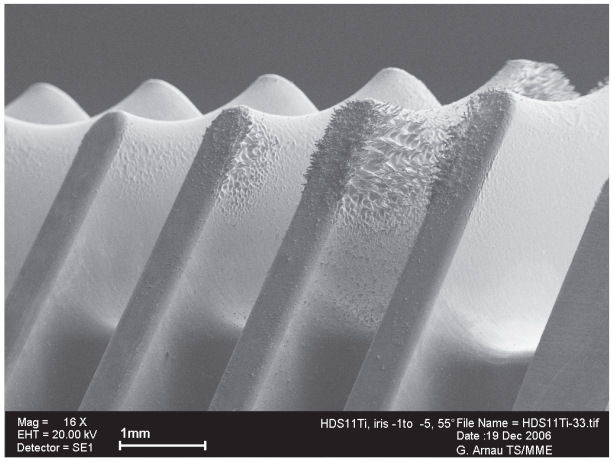

FIG. 12: Damage in a CLIC test structure at high power. This (somewhat uncommon) damage seems to shows the cone structures characteristic of the effects of high electric forces on liquids [39].

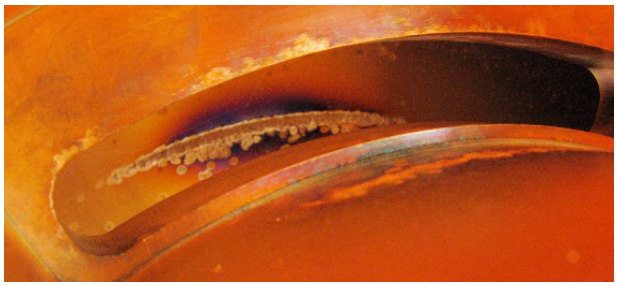

FIG. 13: The interior of the 805 MHz pillbox cavity looking through the coupling slot to see damage on the opposite wall that mirrors the shape of the breakdown pattern on the inside radius of the coupling slot itself. The rf magnetic fields should prevent this damage in the absence of external solenoidal fields.

only atoms involved in the formation of the plasma are copper, and any contaminants such as gasses or other metals would exist at a very low density in the plasma and in subsequent surface damage. This seems to be confirmed by measurements of the spectroscopy of copper arcs. These measurements cover the visible region of the spectrum and not the UV/x-ray region where the the highest power densities of plasma radiation would be expected [17, 48].

VII. MAGNETIC FIELD EFFECTS

Magnetic fields affect the development of the plasma arc. Figure 7 shows that adding an axial magnetic field of 1 T to the OOPIC Pmodel increases the line radiation by a factor of roughly 10 in the first 5 ns of the breakdown event. This assume this is due to some magnetic confinement of the plasma electrons and ions. This would imply that both ion and electron densities would increase by roughly a factor of three only 5 ns into the development of the discharge. This would produce both a faster exponential development of the discharge and perhaps higher power levels deposited on the walls. Modeling the complete development of the discharge will show how the surfaces are affected by magnetic field effects.

The primary effect of strong external solenoidal fields is expected to be the confinement of electrons and ions from the discharge along magnetic field lines. As shown in Fig. 13, we see damage on opposite sides of the cavity that we attribute to these external fields.

Magnetic fields can have other strong, and not well understood, effect on the limiting gradient of an rf structure. It is well known that very high power signals can be transmitted by modest coax cables without breakdown because the circumferential fields are strong enough to prevent electrons from crossing the gap between the center and outer conductor. This effect is called magnetic insulation and this can be studied by varying the angle of the magnetic field with the electric field (which is always normal to the surface).

One diagnostic advantage produced by the magnetic field was that the field emitted electrons, basically pinned to the magnetic field lines, imaged the field emitter pattern on the surface, producing reasonably high resolution images of both the position and enhancement factor (sensitivity to breakdown) on Polaroid film or glass slides. During breakdown events, this technique may not be practical, however, as the power in these beams becomes much larger and can damage windows and other components [26, 27].

Measurements made in two different cavity geometries, an open cell [26] and a short pillbox [27], have produced somewhat conflicting results during an extensive test period. The open, six cell cavity was able to reach essentially the same fields with and without solenoidal fields up to about 4.5 T, however the short pillbox was not able to reach the same electric field in the presence of magnetic fields from 0.5 - 4 T [26, 27]. Both cavities seemed to require a certain amount of re-conditioning each time the B field was increased, and again when it was turned off, in order to reach the maximum possible electric field, as shown in Fig 14. There are a number of explanations for these effects and an experimental program is underway to help understand the mechanisms involved. The geometries of the two cavities are not the same, which implies that some magnetic insulation could be involved, or perhaps the magnetic field helps confine the plasma to a smaller area, increasing the local surface damage. On the other hand, magnetic forces could alter the dynamics of the charged molten metal which seems to be responsible for the damage, and future triggers, in the cavity.

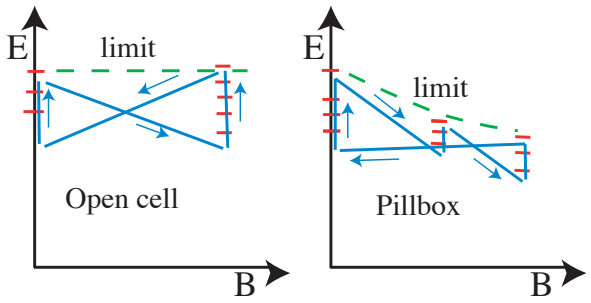

FIG. 14: the tuning path followed to determine the maximum gradient as a function of B in the open cell and pillbox cavities.

VIII. HIGH PRESSURE GAS

Recently, there has been an effort to look at the breakdown properties of cavities operating at high gas pressure [49]. This work continues a study that started in about 1900 when Michaelson and Millikan initially identified two causes of electrical breakdown, avalanches of the gas and breakdown of the surface [7, 9].

Gas breakdown at high electric fields is a function only of the ratio E/p, where E and p are the electric field and pressure. Under most laboratory conditions, this term is modified by some factor which depends on the geometry of the structure used, since the dimensions of the electron avalanche can under many circumstances, exceed the dimensions of the structure. Except for prompt radiation induced resistivity, the properties of gas breakdown have been understood for many years and are not considered here.

In the breakdown model we are describing, high fields at asperities will still cause fragmentation and ionization of material released from the surface. The presence of gases in this environment can slow down and attenuate the field emitted electrons, affecting the plasma creation and breakdown properties. The process is a function of how the fields accelerating electrons and the gas slowing them down interact with the electrons emitted from the surface. It is useful to discuss air as a representative gas, as the energy loss, dE/dx, for air has been carefully measured over a large energy range and the general features we will discuss are common to all gasses [50]. Nevertheless, other gasses are also relevant such as SF_6 and H_2, used to prevent waveguide breakdown and in systems proposed for cooling muons.

The accelerating and decelerating forces in gasses with surface asperities and applied electric fields are shown in Fig 15. The accelerating field always starts about 7 - 10 GV/m and drops like $1/r^2$ so the energy gained by the particle is on the order of Er, where E is the surface field at the asperity and r is the radius. The shape of the electric field vs energy curve is thus a function of the asperity radius. The drag term due to the gas is proportional to pressure.

At high energies, under almost all conditions, the acceleration term must be greater than the deceleration term, thus any electron that can somehow achieve an energy sufficiently high to be in this range will essentially be ballistically accelerated. For most gasses this energy seems to be around 1 keV, which is too hign to be accessible in normal breakdown events. Ionization by high energy particles, however, produce a significant fraction of electrons above this energy. High pressure cavities can operate at densities that are very similar to those of hydrogen bubble chambers. The $\sim$ 1 keV threshold also seems to be the energy that generates the bubbles in bubble chambers, so the production of these electrons by high energy beams, has been extensively studied [51].

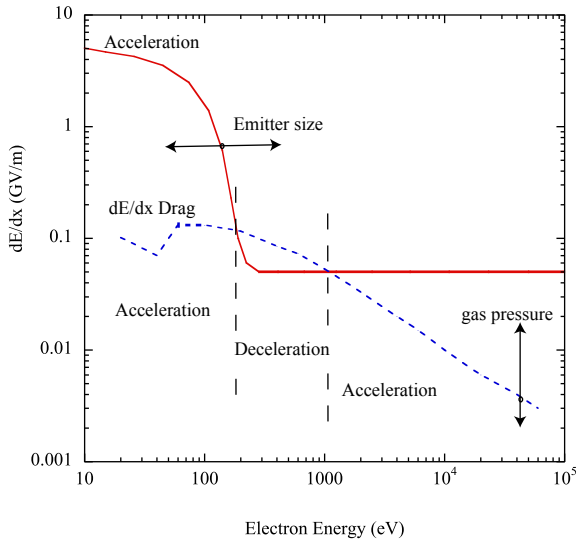

FIG. 15: The acceleration and drag terms under breakdown conditions. The acceleration term is determined by the local surface field whose extent is comparable to the radius of the asperity, where it slowly drops to the average surface field of the cavity. The drag term is determined by the atomic properties of a given gas and its pressure. This plot assumes a 30 nm spherical asperity with a surface field of 7 GV/m using air at 20 atmospheres (a density of 24 mg/cm^3) as an insulating gas [50]. Other relevant gasses, (H_2 and SF_6), would be expected to have quite different drag for low energy electrons, but similar properties (at comparable densities) for high energy electrons.

IX. EXTINGUISHING THE ARC

In the model described here, the plasma would exist as long as there are electric fields in the structure, and the gradients required to maintain the arc may be much less than those required to create it. If the principle energy loss mechanism is shorting of the cavity by plasma electrons, this process would occur as long as the shorting mechanism was efficient. In this respect standing and traveling wave cavities may be different, as standing wave

cavities would discharge their energy to a level where shorting was less efficient, whereas arcs in traveling wave structures would see essentially the same fields until the power was terminated.

During the arc the surface would be expected to get hot, and outgas whatever was on the surface, and there would be a fairly long time constant (seconds) for more or less complete recombination of the plasma ions. This would prohibit power from being applied to the cavity.

X. PULSED HEATING IN COPPER STRUCTURES

With the comparatively low frequency structures used in the muon cooling program, we expect that the primary cause of damage in the internal surface of a cavity is either present when the structure was first powered, or created by breakdown events tracing their history back to these original defects. In higher frequency cavities, there is another effect that can produce surface damage called "pulsed heating" [52]. At high frequencies and high gradients, the Ohmic heating caused by the cavity currents, which penetrate only about 500 nm into copper at 10 GHz, can heat up the walls of the cavity on the order of 100 K during pulses of $\sim$0.1 μsec. This heating pulse penetrates somewhat deeper into the walls than the current pulse, but it is essentially a surface phenomenon. The differential, repetitive, surface heating, and the thermal expansion which accompanies it, produces stresses and fatigue, since the material is free to move only perpendicular to the surface, and cannot expand in the plane of the surface. The phenomenon has been described by Pritzkau and Siemann, [52]..

The temperature variation in the wall should be proportional to Ohmic heating. For a cavity of radius r, this term is, $\rho I^2/2\pi r\delta$, where the wall current is $I \sim \omega EA$, the frequency, $f = 2\pi\omega \sim 1/r$,the area of the pillbox end is $A = \pi r^2$, and ρ is the resistivity. Since the skin depth is $\delta \sim \sqrt{1/f} \sim \sqrt{r}$, we find that surface heating, for pulses of the same length, is proportional to $E^2 f^{-1/2}$. Thus low electric fields and short pulses produce the least wall heating. Wall heating can be further reduced by using materials with high electrical conductivity and high specific heat.

While it is sometimes assumed that the regions of high field and high surface currents are widely separated in pillbox cavities, the highest current densities in pillbox cavities are located on the ends of the cavity. and electric fields high enough to cause breakdown are present at quite large radii, if large enhancement factors exist. Thus starting with a perfect cavity surface does not guarantee that a cavity can be breakdown free, however in most cases breakdown occurs at irises.

Pulse heating develops stress in the top layers of the surface due to differential heating and expansion driven by surface currents. Experimental data from surfaces exposed to these surface currents shows both damage that is visible to the eye, and microscopic cracks and compressive strain visible microscopically [52]. At the nano level we expect that this damage would take place suddenly, in microshocks rather than slow plastic flow. With stresses comparable to the tensile strength of the metal involved, we expect that some microparticulates will be created, as they are when macroscopic surfaces move against each other. With large forces and small particulates these particles could travel across the structures, from regions with low electric fields to regions with high fields, causing breakdown driven by local electric fields rather then magnetic fields. As described in an earlier paper, surface currents can produce high gradients at grain boundaries, which would also contribute to local stresses [53].

XI. SUPERCONDUCTING RF

Warm structures, principally made of copper, are comparatively rugged objects which can survive significant perturbations on the surface, and are capable of burning off asperities which would limit the gradient of the system. Superconducting structures, on the other hand, use only the top 40 nm of the material, some of which is occupied with surface oxide, and the conduction is carried by Cooper pairs of electrons that are coupled by an interaction with a binding energy of 1.5 mV. The systems operate at temperatures of 2 - 4 K, and are sensitive to thermal fluctuations that significantly perturb this environment. Thus, we find that whereas copper structures have basically one mechanism which limits the gradient, superconductors, being more delicate, seem to have almost a dozen gradient limiting mechanisms [54].

One of these mechanisms, used to advantage in High Power Processing (HPP), seems to be essentially the sort of breakdown arc that we are describing here [31]. Although in modern cavities particulate contamination is generally responsible, field emitters can also limit the performance of a structure due to dark current beams heating up either the emitter or the region of the cavity where the beams hit the wall, showing that local regions of high field exist. In some cases these emitters seem to have local surface fields around 4 GV/m [18]. These asperities can sometimes be "burned off" with short, high power pulses, which presumably increase the local gradient to the point where breakdown events, essentially like those described here, occur.

Since superconductors cannot absorb heat without going normal, a hot plasma would be expected to make the area surrounding the breakdown event normal, cutting it off from the supercurrents which drove the cavity oscillations. Nevertheless, the electric fields which drive the arcs would be present, and the arc would proceed in a similar way. A comparison between the timescales of breakdown events in normal and superconducting structures would be useful.

XII. CURING BREAKDOWN

The arguments presented in this paper imply that local smoothing seems to be the best way of producing cavities that operate at higher gradients. Field emission, while not required as a part of the trigger mechanism, seems to be responsible for the initial ionization of material which initiates the arc, but it is the local electric field, a function of the cavity parameters and wall microstructure, that are responsible for starting the breakdown process. In order to prevent breakdown events, cleanliness and smoothness of the walls are the only external variables that can affect this process. A variety of polishing and cleaning methods seem useful, together with the use of clean room technology. In addition to these methods, Atomic Layer Deposition (ALD) has the ability to conformally coat asperities to increase their local radii, decreasing the local electric fields they would cause. This technology may be promising for high frequency structures which are too small or complex to be polished by other methods.

While pulse heating can be a serious problem at high frequencies, it may be that lower frequencies would produce lower levels of heating. Atomic Layer Deposition (ALD) should also be able to produce structures which can carry current in thin layers separated by insulators which should function as thermal sinks.

XIII. DC ARCS

This model should also be relevant to the study of DC arcs [14, 42]. Breakdown is a very common phenomenon that occurs in air whenever electrical contact is made at more than 10 - 20 V [7, 9]. We expect that DC arcs would be driven and controlled by the same mechanisms as rf arcs, with a number of differences. The arcs should develop much faster than rf arcs because the electric field is always present and has the right polarity. We would also expect that the constant polarity should require a lower trigger threshold, because the phenomenon would be continuously driven.

It is interesting to consider breakdown of surfaces at high positive potential (as in APT systems) or breakdown of free particles suspended, perhaps inertially, away from a source of electrons. It is known that APT samples, charged positively, frequently fail, (mini-flashes), and we expect this would be due to tensile stress followed by field emission currents from a large fragment, followed by Coulomb explosion, similar to rf arcs.

XIV. CONCLUSIONS

This paper presents an outline of how high surface fields could fracture the surface of field emitting asperities in an rf cavity to form a plasma, and this plasma could provide sufficient electrons which would melt the surface locally and short the cavity in a timescale of a few ns. The model can, in principle, describe all aspects of the growth of the plasma, and the mechanisms that drive and control this growth. We are refining, extending and improving this model to make it more precise and applicable to a wider range of rf structures.

In an earlier paper we have described how an equilibrium between the stored energy of the structure and the surface damage can determine many of the properties of the system [18]. In this paper we have shown how the parameters of the arc are determined by the rf environment. For example, we show the amount of material expelled from the surface can determine if an arc will occur or not. We have described a number of trigger mechanisms and adopted fracture as the most interesting one for this study. We have shown what mechanisms drive the development of the discharge, and shown how space charge, electron kinetics and bulk heating can control the rate of the development of the discharge. We have compared predictions of the model with experimental measurements of the rise time of the x ray pulse with good agreement. We have discussed why discharges can vary in power from one to another. We have shown how the plasma environment provides a mechanism for accelerating droplets of metal (particulates). We have shown how magnetic fields can influence discharge development and maximum operating fields. We have shown how pulse heating might generate real breakdown events. We have shown how the mechanisms we discuss affect high pressure cavities, superconducting systems and DC structures of different polarities. We also show the range of different techniques to cure this problem.

While this paper is primarily an outline of the mechanisms involved, it demonstrates that these mechanisms are capable of driving very fast avalanche processes that can interfere with or end the normal operation of the cavity. More detailed analysis of different mechanisms described here is underway and we expect to be able to provide more precise results in the future. Where possible we compare this model with a variety of experimental data from various sources. We believe all aspects of this model are experimentally accessible and a more detailed comparison of the model and experimental data would be very productive.

XV. ACKNOWLEDGEMENTS

We would like to thank the staff of the Accelerator and Technical Divisions at Fermilab for supporting and maintaining our experimental program in the MTA experimental area. The cavity was constructed by D. Li, and the staff of LBL. During the evolution of this work, we have had continual interactions with members of the Neutrino Factory and Muon Collider Collaboration, (NFMCC), the Muon Collider Task Force, (MCTF), at Fermilab, the Muon Ionization Cooling Experiment (MICE) at Rutherford, and with K. Yonahara and R.

Johnson of Muons Inc. R. Palmer of BNL has taken an active interest in this subject with many useful suggestions. This work is supported by the Department of Energy Office of High Energy Physics, at Argonne by Contract No. DE-AC02-06CH11357. The work of Tech-X personnel is funded by the Department of Energy under Small Business Innovation Research Contract No. DE-FG03-02ER83554.

[1] D. Neuffer, $\mu^+ - \mu^-$ *Colliders*, CERN Yellow Report CERN-99-12, (1999).
[2] S. Geer and M.S. Zisman, Prog. in Part and Nucl. Phys. **59** (2007) 631.
[3] M. S. Zisman, *Status of the international Muon Ionization Cooling Experiment (MICE)*, Proc. of PAC07, June 25-29, 2007, Albuquerque, New Mexico, USA, p2996.
[4] http://public.web.cern.ch/public/en/Research/CLIC-en.html
[5] http://www.linearcollider.org/cms/
[6] R. W. Wood, Phys. Rev. **1**, 1, (1897).
[7] R. F. Earhart, Phil. Mag. 1, 147, (1901).
[8] Lord Kelvin, Phil. Mag, 8, 534 (1904), also, *Mathematical and Physical Papers, Vol. VI, Voltaic theory, Radioactivity, Electrions, Navigation and Tides, Miscellaneous*, Cambridge University Press, Cambridge, (1911), p211.
[9] G. M. Hobbs, Phil. Mag., 10, 617 (1905).
[10] R. A. Millikan, *Autobiography*, Prentice-Hall, New York, (1950).
[11] L. L. Laurent, *High Gradient rf Breakdown Studies*, University of California, Davis, PhD Thesis, (2002).
[12] D. Alpert, D. A. Lee, E. M. Lyman and H. E. Tomaschke, J. Vac. Sci. Technol. 1, 35, (1964).
[13] F. R. Schwirzke, IEEE Trans. on Plas. Sci., **19**, 690, (1991)
[14] G. A. Mesyats, *Explosive Electron Emission*, URO Press, Ekaterinberg, Russia, (1998).
[15] P. B. Wilson, AIP Conf. Proc. **877**, 27 (2006).
[16] R. Latham, *High Voltage Vacuum Insulation*, Authorhouse, UK, DS, (2006).
[17] V. A. Dolgashev, S. G. Tantawi, C. D. Nantista, Y. Higashi, T. Higo, Proceedings of 2005 Particle Accelerator Conference, Knoxville, Tenn (2005).
[18] A. Hassanein, Z. Insepov, J. Norem, A. Moretti, Z. Qian, A. Bross, Y. Torun, R. Rimmer, D. Li, M. Zisman, D. N. Seidman, and K. E. Yoon, Phys. Rev. STAB **9** 062001 (2006).
[19] D. L. Bruhwiler, R. E. Giacone, J. R. Cary, J. P. Verboncoeur, P. Mardahl, E. Esarey, W. P. Leemans and B. A. Shadwick, Phys. Rev. ST-Acc. & Beams, **4**, 101302, (2001).
[20] Tech-X, Inc., Boulder CO (2008).
[21] C. Nieter and J. R. Cary, J. Comput. Phys, **196**, 448, (2004).
[22] R. H. Fowler and L. Nordheim, Proc. Roy Soc **A119** 173 (1928).
[23] I. Brodie, and C. A. Spindt, Adv. in Electron. and Electron. Physics, **83**, (1992) 1.
[24] M Belkacem, F. Jegi. P.-G. Reinhard, E. Suraud and G. Zwicknagel, Phys. Rev. A, **73** 051201(r), (2006).
[25] P.-G. Reinhard and E. Sauraud, *Introduction to Cluster Dynamics*, Wiley, New York, (2003).
[26] J. Norem, V. Wu, A. Moretti, M. Popovic, Z. Qian, L. Ducas, Y. Torun and N. Solomey, Phys. Rev. STAB, **6**, 072001, (2003).
[27] A. Moretti, Z. Qian, J. Norem, Y. Torun, D. Li, M. Zisman, Phys. Rev. STAB, **8**, 072001 (2005).
[28] J. P. Barbour, W. W. Dolan, J. K. Trolan, E. E. Martin and W. P. Dyke, Phys. Rev. **92**, 45, (1953)
[29] R. Feynman, T. E. Leighton and M. Sands, *Feynman Lectures on Physics, Vol II*, Addison Wesley New York (1963) Section 6-11.
[30] L. Nilsson, O. Groening, P. Groening, O. Kuettel, and L. Schlapbach, J. Appl. Phys, **90,2**, 768, (2001)
[31] H. Padamsee, J. Knobloch, T. Hays, *RF Superconductivity for Accelerators*, Wiley-Interscience, New York, (1998).
[32] G. Mueller, University of Wuppertal, Private Communication, (2007).
[33] D. Lysenkov, and G. Mueller, Int. J. Nanotech. **2**, 239, (2005).
[34] W. P. Dyke, and J. K. Trolan, Phys. Rev. **89** (1953) 799.
[35] J. Norem, D. Huang, P. Stoltz, S. Veitzer, *A General Model of High Gradient Limits*. Proceedings of PAC07, Albuquerque, June 25-29, 2007, USA, 2236-2239, (2007).
[36] N. E. Dowling, *Mechanical Behavior of Materials*, Prentice Hall, Upper Saddle River, NJ, (1999).
[37] Z. Insepov, J. H. Norem, A. Hassanein, Phys. Rev. STAB **7**, 122001 (2004).
[38] K. T. Hong, J. K. Lee, S. W. Nam, J. Mat. Sci. **23** 1569, (1988).
[39] W. Wuensch and G. Arnau-Izquierdo, CERN, private communication (2008)
[40] M. K. Miller, *Atom Probe Tomography. Analysis at the Atomic Level* Kluwer Academic/Plenum Publishers, New York, (2000).
[41] L. Rayleigh, Phil. Mag. **14**, 184, (1882)
[42] H. J. G. Gielen and D. C. Schram, IEEE Trans. on Plas. Sci., **18,1**, 127, (1990).
[43] D. Mosher, Phys. Rev. A, **10**, 2330, (1974).
[44] , K. L. Jensen, P. G. O'Shea, D. F, Feldman, App. Phys. Lett. **82**, 3867 (2002).
[45] D. M. Ritson, *Techniques of High Energy Physics*, Interscience, New York, (1961).
[46] V. Gandia and E. Lopez-Baeza, J. Phys. E: Sci. Instrum., **21**, 757, (1988).
[47] T. Matsumoto, H. Fujii, T. Ueda, M. Kamai and K. Nogi, Meas. Sci. Technol. **16**, 432, (2005).
[48] J. Kovermann at the CLIC Breakdown Workshop, CERN (2008), http://indico.cern.ch/ conferenceDisplay.py?confId=33140
[49] P. Hanlet, M. Alsharo'a, R. E. Hartline, R. P. Johnson, M. Kuchnir, K. Paul, C. M, Ankenbrandt, A. Moretti, M. Popovic, D. M. Kaplan, K. Yonehara, Proceedings of EPAC 2006, Edinburgh, Scotland, (2006)
[50] A. Cole, Rad. Res., **38**, 7, (1969)
[51] F. Seitz, Phys. of Fluids. **1,1**, 2, (1958).
[52] D. P. Pritzkau and R. H. Siemann, Phys. Rev. ST Accel. Beams 5, 112002 (2002).
[53] J. Norem, Z. Insepov, and I. Konkashbiaev, Nucl. Instr

and Meth. in Phys. Res. A **537** (2005) 510.
[54] J. Norem and M. Pellin, 13th International Workshop on RF Superconductivity, Peking University, Beijing, China, Oct. 14-19, (2007).